are shown in Figure 7. It is remarkable that throughout the RFID bandwidth the measured return loss is less than −10 dB.

The measured resonant frequency is greater than the numerical model one indicating that the FR-4 relative permittivity of the prototype is slightly less than 4.4. Simulations were performed in order to match the resonant frequencies and indirectly estimate the FR-4 permittivity. This procedure is adopted in Ref. 17. The resonant frequency of the measurement and the model one matched considering $\varepsilon_r' = 4.38$. To match experimental curves with numerical simulations curves is a classical method to calculate the electromagnetic properties [18].

The gain is measured at the point $\theta = 0°$ and $\varphi = 0°$. Figure 8 shows the experimental data and results from numerical model. It was performed simulations for $\varepsilon_r' = 4.38$ (obtained from Fig. 7) considering tan $\delta = 0.017$ and tan $\delta = 0.027$ (the smallest and biggest values to loss tangent found in the Refs. 6,13,19,20 and in the manufactures datasheets). The gain measured has good accuracy taken into account the FR-4 uncertainties in its loss tangent.

5. CONCLUSION

In this article, a systematic methodology is proposed to design a low-cost MPA for RFID readers devices. The use of FR-4 material as a substrate greatly decreases the cost of antenna manufacturing. Nevertheless, it introduces some difficulties in the project. The low radiation efficiency was one of them, which is reduced by increasing the thickness of the substrate. Difficulty also arises due to the inaccuracy of the FR-4 electromagnetic properties, but experimental results show that the return loss and gain present required values. At last, the DE multiobjective optimization algorithm is applied in order to obtain a good performance to antenna and respect the available volume to antenna construction.

REFERENCES

1. K.V.S. Rao, P. Nikitin, and S. Lam, Antenna design for UHF RFID tags: A review and a practical application, IEEE Trans Antennas Propag 53 (2005), 3870–3876.
2. J.Z. Huang, P.H. Yang, W.C. Chew, and T.T. Ye, A novel broadband patch antenna for universal UHF RFID tags, Microwave Opt Technol Lett 52 (2010), 2653–2657.
3. L. Ukkonen, M. Schaffrath, D. Engels, L. Sydanheimo, and M. Kivikoski, Operability of folded microstrip patch-type tag antenna in the UHF RFID bands within 865-928 MHz, IEEE Trans Antennas Wireless Propag Lett 5 (2006), 414–417.
4. I. Mayordomo, R. Berenguer, A. Garcia-Alonso, I. Fernandez, and I. Gutierrez, Design and implementation of a long-range RFID reader for passive transponders, IEEE Trans Microwave Theory Tech 57 (2009), 1283–1290.
5. Z.-J. Tang, J. Zhan, and H.-L. Liu, Dual-resonance compact circularly polarized reader antenna for UHF RFID applications, Microwave Opt Technol Lett 54 (2012), 2531–2533.
6. S. Pflaum, P. Le Thuc, G. Kossiavas, and R. Staraj, Performance enhancement of a circularly polarized patch antenna for radio frequency identification readers using electromagnetic band-gap ground plane, Microwave Opt Technol Lett 55 (2013), 1599–1602.
7. I. Bahl, R. Garg, A. Ittipiboon, R. Garg, and P. Bhartia, Microstrip antenna design handbook, Artech House, Norwood, MA, 2001.
8. C.A. Balanis, Antenna theory: Analysis and design, Wiley-Interscience, Hoboken, NJ, 2005.
9. W. Hong, K.H. Baek, and A. Goudelev, Multilayer antenna package for IEEE 802.11ad employing ultralow-cost FR-4, IEEE Trans Antennas Propag 60 (2012), 5932–5938.
10. R. Storn and K. Price, Differential evolution—A simple and efficient heuristic for global optimization over continuous spaces, J Global Optim 11 (1997), 341–359.
11. X.L. Travassos, A.C. Lisboa, and D.A.G. Vieira, Design of meander-line antennas for radio frequency identification based on multiobjective optimization, Int J Antennas Propag 60 (2012).
12. A.C. Lisboa, D.A.G. Vieira, J.A. Vansconcelos, R.R. Saldanha, and R.H.C. Takahashi, Decreasing interference in satellite broadband communication systems using modeled reflector antennas, IEEE Trans Magnet 44 (2008), 958–961.
13. M. Ammann, A comparison of some low cost laminates for antennas operating in the 2.45 GHz ISM band, IEE Colloq in Low Cost Antenna Technol (1998), 3/1–3/5.
14. D.C.Nascimento, R. Schildberg, and J. C. S. Lacava, Design of low-cost microstrip antennas for glonass applications, In: Progress in Electromagnetics Research Symposium, 2008, pp. 199–202.
15. E. Clement Mbinack and D. TonyeBajon, Microstrip-line theory and experimental study for the characterization of the inset-fed rectangular microstrip-patch antenna impedance, Microwave Opt Technol Lett 57 (2015), 514–518.
16. High Frequency Structure Software, Ansys HFSS software, 2014. [Available online at: http://www.ansys.com]. Last accessed June 12, 2014.
17. P.R. Katiyar, M.M. Shafiei, and W. Mahadi, Characterizing FR-4 dielectric constant using antenna resonant frequency, Microwave J 48 (2005), 96–102.
18. R.A. Fenner and S. Keilson, Free space material characterization using genetic algorithms, In: International Symposium on Antenna Technology and Applied Electromagnetics, 2014, pp. 1–2.
19. A. Ege Engin, Extraction of dielectric constant and loss tangent using new rapid plane solver and analytical debye modeling for printed circuit boards, IEEE Trans Microwave Theory Tech 58 (2010), 211–219.
20. A.R. Djordjevic, R.M. Biljic, V.D. Likar-Smiljanic, and T.K. Sarkar, Wideband frequency-domain characterization of FR-4 and time-domain causality, IEEE Trans Electromagn Compat 43 (2001), 662–667.

EXTREMELY WIDEBAND PRINTED MONOPOLE ANTENNA WITH DUAL REJECTION BANDS

Zhale Amiri,[1] Sima Movagharnia,[2] Masoume Masoumi,[3] Majed Shokry,[1] and Bal S. Virdee[4]

[1] Young Researchers and Elite Club, Urmia Branch, Islamic Azad University, Urmia, Iran; Corresponding author: zhale.amiri@gmail.com

[2] Department of Electrical Engineering, Urmia University, Urmia, Iran

[3] Department of Electrical Engineering, Urmia Branch, Islamic Azad University, Uremia, Iran

[4] Faculty of Life Sciences and Computing Center for Communications Technology, London Metropolitan University, London, UK

Received 15 August 2015

ABSTRACT: *An extremely wideband (EWB) microstrip antenna is presented that is designed with band rejection characteristics at C and WLAN bands. This is achieved by embedding inside the inverted triangular shaped patch a pair of L-shaped slits that have been rotated by ±90° so that they are horizontal and downward facing, and topping the patch with an arrow-shaped strip. The feedline to the patch also needs to be backed with a trapezoid shaped ground-plane. The center frequency of the notched bands can be easily controlled by altering the parameters of the slits and arrow-shaped strip. The low-profile antenna essentially radiates omni-directionally and has a measured impedance bandwidth of 18.9 GHz (2.9–21.8 GHz) with a VSWR ≤ 2, except at the two rejection bands. The antenna has an average gain > 3 dBi.* © 2016 Wiley Periodicals, Inc. Microwave Opt Technol Lett 58:908–911, 2016; View this article online at wileyonlinelibrary.com. DOI 10.1002/mop.29694

Key words: *microstrip antenna; ultra-wideband antenna; dual band notch*

1. INTRODUCTION

Ultra-wideband (UWB) technology is increasingly becoming a favored choice for short-range and high-speed (>100 Mbps) indoor data communications ever since the Federal Communications Commission (FCC) released it for commercial applications [1–5]. UWB systems require a single antenna that cover its spectrum (3.1–10.6 GHz) and needs to be low-profile and sufficiently small for system integration. Hence, printed monopole antennas have attracted great interest for UWB systems as they possess properties of wide impedance bandwidth, ease of fabrication using conventional MIC technology and therefore economic for mass production, and exhibit acceptable radiation properties [2–5]. Moreover, UWB systems need to coexist with other wireless narrowband standards such as WLAN (5.15–5.35 GHz and 5.725–5.825 GHz), WiMAX (3.3–3.6 GHz), and other C-band (3.7–4.2 GHz) systems, which are likely to interfere with the operation of UWB systems as they transmit at a significantly higher power level than UWB systems. Various band-notched UWB antennas have been recently proposed using different techniques but their main deficiency is relatively large physical size that prevents system miniaturization [3–5].

In this letter, a novel low-profile printed monopole UWB antenna is presented with dual notched band characteristics to mitigate interfering signals. By modifying the key parameters of the slits and arrow-shaped strip enables easy control of the center frequency of the notched bands. Compared to some previously reported antennas it is more compact in size and has a wide impedance bandwidth.

2. ANTENNA STRUCTURE

The configuration of the proposed antenna and optimized dimensions are shown in Figure 1.

The antenna occupies a volume of $30 \times 30 \times 1.6$ mm^3. The 50-Ω feedline is an effective impedance transformer having a width and length of 2.8 mm and 12.9 mm, respectively, and is connected to an SMA connector. Figure 2 shows the steps employed to implement the proposed antenna structure. As shown in Figure 2, to achieve a wider impedance bandwidth it is necessary to truncate the ground-plane into the shape of a trapezoid resting on a rectangular base, and cutting a semi-circular notch in the ground-plane near the neck of the patch. To obtain notched band function at the WLAN band a pair of L-shaped slits are created at the two sides of the inverted triangular patch, which have been rotated by ±90° so that they are horizontal and downward facing. The patch is topped with an arrow-shaped strip to create a notched band at C-band.

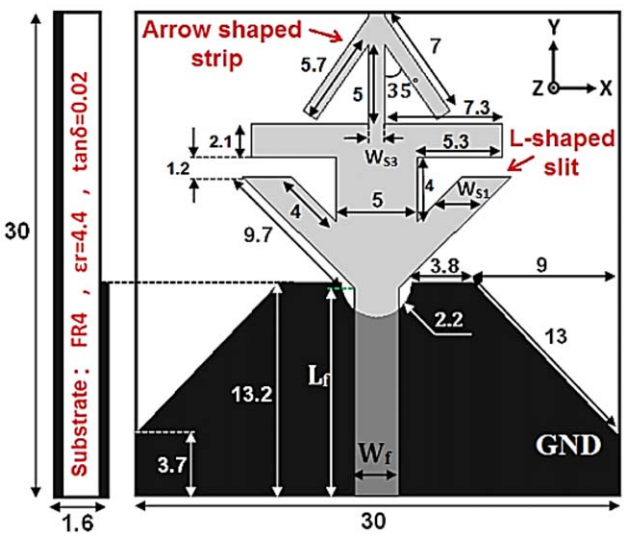

Figure 1 Geometry of the proposed antenna (optimized dimensions in millimeter). [Color figure can be viewed in the online issue, which is available at wileyonlinelibrary.com]

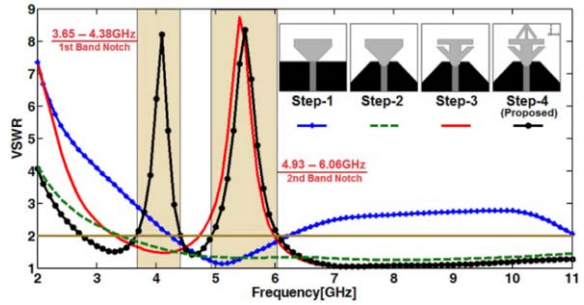

Figure 2 VSWR of various evolution steps taken to realize the finalized design. [Color figure can be viewed in the online issue, which is available at wileyonlinelibrary.com]

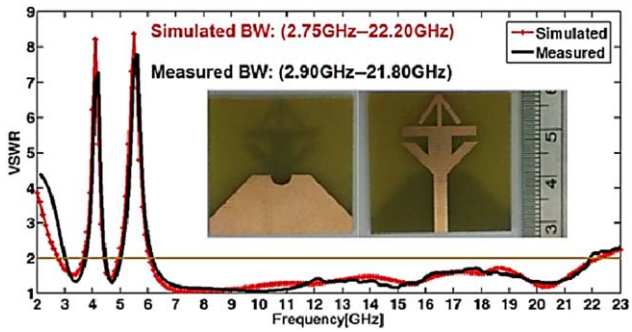

Figure 3 Numerical and experimental VSWR curve of the fabricated antenna prototype. Inset is the photograph of the proposed antenna. [Color figure can be viewed in the online issue, which is available at wileyonlinelibrary.com]

The simulated and measured VSWR of the proposed antenna is shown in Figure 3. Inset in the graph is a photograph of the fabricated prototype antenna. The measured VSWR of the antenna stretches from 2.90 to 21.80 GHz for a VSWR ≤ 2, which was measured using Agilent 8722ES VNA. The antenna performance exceeds the UWB defined by FCC. The two notched bands between 3.65 and 4.38 GHz and 4.93 and 6.06 GHz effectively reject signals at C and WLAN bands, respectively. There is excellent agreement between the simulated and measured results.

TABLE 1 Parametric Study on W_{S1} and W_{S3}

Parameter	Magnitude (mm)	1st Notch BW (GHz)	2nd Notch BW (GHz)
W_{S1}	3 (optimized)	3.65–4.38	4.93–6.06
	3.5	3.56–4.31	5.03–6.26
	4.5	3.43–4.08	5.15–6.69
W_{S3}	1 (optimized)	3.65–4.38	4.93–6.06
	1.2	3.79–4.63	5.02–6.06
	1.4	3.85–4.81	5.06–6.06

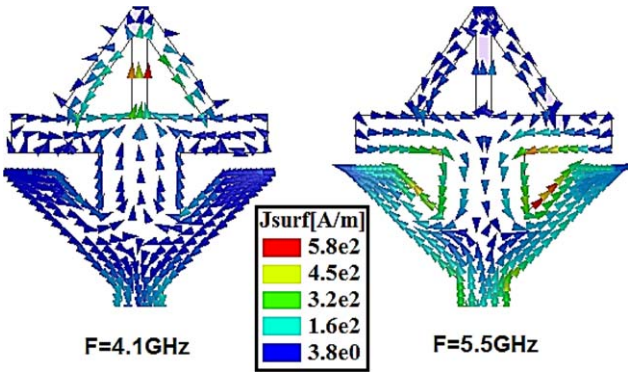

Figure 4 Current distributions over the antenna at the notch frequencies. [Color figure can be viewed in the online issue, which is available at wileyonlinelibrary.com]

3. SIMULATION AND MEASUREMENT RESULTS

Parametric analysis was done using Ansoft High Frequency Structure Simulator (HFSS ver.11) to gain a deeper insight of the antenna structure. It reveals that the center frequency of the dual notched bands can be simply altered by changing the dimensions of the L-shaped slits and arrow-shaped, in particular primarily parameters W_{S1} and W_{S3}.

As is evident in Table 1, by increasing W_{S1} from 3 mm to 4.5 mm, with other parameters kept fixed, the first notched band moves toward lower frequencies while the second band shifts toward higher frequencies. The W_{S3} parameter mainly determines the frequency location of the first notched band. Upon increasing W_{S3} with other parameters remaining unchanged, the first notched band moves to higher frequencies, but the position of the second notched band remains essentially insensitive to the variation of W_{S3}.

The current distributions at 4.1 and 5.5 GHz of the optimized antenna design is shown in Figure 4. At 4.1 GHz, current is mainly distributed at the interior edge of the arrow-shaped strip with length L_{notch1}= 18 mm, which is nearly 0.25λ at 4.1 GHz. Similarly at 5.5 GHz, current mainly exists along the L-shaped slit with length L_{notch2}= 14 mm, which is 0.25λ at 5.5 GHz. Because of the symmetrical feature of the two rejection band (C and WLAN bands) structures the radiation fields generated by the oppositely directed currents cancel each other out at the notch frequencies.

The measured gain response, shown in Figure 5, exhibits two sharp attenuations characteristics centered at 4.25 GHz and

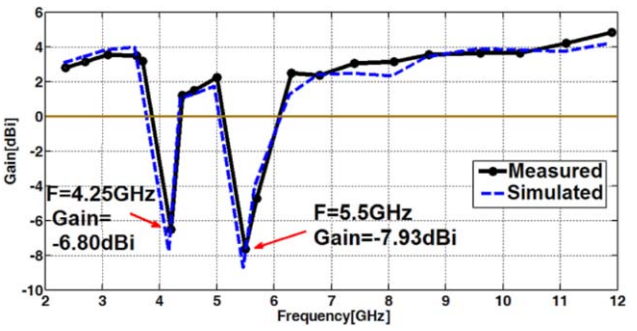

Figure 5 The measured and simulated antenna gain versus frequency. [Color figure can be viewed in the online issue, which is available at wileyonlinelibrary.com]

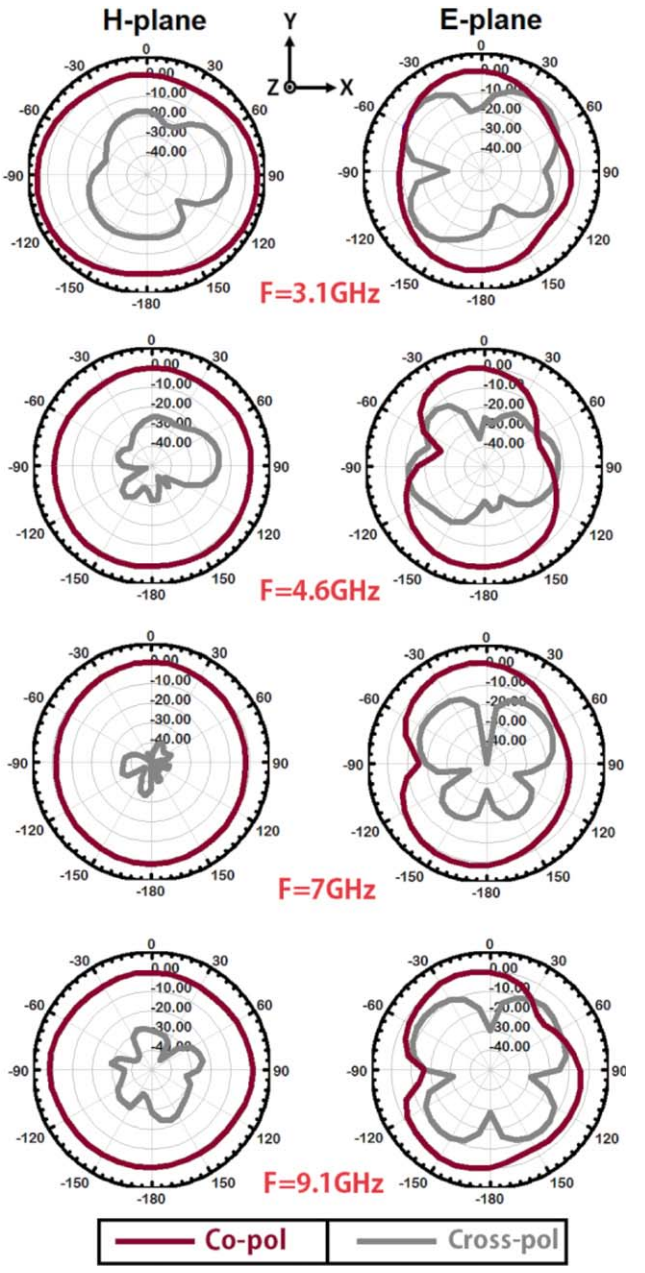

Figure 6 Radiation patterns of the proposed antenna. [Color figure can be viewed in the online issue, which is available at wileyonlinelibrary.com]

5.55 GHz, showing the effectiveness of the notched bands. The radiation patterns of the proposed antenna are shown in Figure 6 at 3.1 GHz, 4.6 GHz, and 9.2 GHz in *H*-plane (*xz*-plane) and

TABLE 2 Comparison of the Proposed UWB Antenna with Previously Reported UWB Antennas

Antenna	Antenna Area (mm^2)	Notched-Band	Impedance Bandwidth (%)
Ref. 3	52 × 40	Dual	114.2
Ref. 4	38 × 35	Dual	128.7
Ref. 5	34 × 30	Dual	124.3
Ref. 6	33 × 29.6	Dual	105.3
Ref. 7	34 × 34	Dual	120
Proposed	30 × 30	Dual	153.0

E-plane (*yz*-plane). The fabricated antenna exhibits an omni-directional radiation pattern across the UWB frequency band in *H*-plane and approximately omni-direction in the *E*-plane.

Table 2 compares the characteristics of the proposed antenna with other UWB antennas with dual notched bands. The table shows the proposed antenna is physically smaller (30×30 mm^2) and has largest impedance bandwidth of 153%.

4. CONCLUSION

A novel printed monopole antenna is described with extremely wideband characteristics for UWB applications. The antenna includes notched-band to reject interfering signals in C and WLAN bands, which are realized by embedding a pair of horizontally rotated L-shaped slits within an inverted triangular shaped patch that is topped with an arrow-shaped strip. The antenna has an extremely wide impedance bandwidth of 153% and radiates essentially omni-directionally in both *E*- and *H*-planes. The average gain of the antenna >3 dBi and the center frequency of the notched bands can be easily controlled by altering the parameters of the slits and arrow-shaped strip. Compared to other UWB antennas with dual notched bands the proposed antenna is more compact.

ACKNOWLEDGMENT

The authors like to thank the Antenna Measurement Laboratory at Iran Telecommunication Research Center (ITRC) for fabricating and testing the antenna presented in this paper.

REFERENCES

1. FCC First Report and Order on the Ultra-wideband Technology, Washington, DC, 2002.
2. S. Mohammadi, J. Nourinia, C. Ghobadi, and M. Majidzadeh, Compact CPW-fed rotated square-shaped patch slot antenna with band-notched function for UWB applications, Electronic Lett 47 (2011), 1307–1308.
3. W.C. Kim and W.G. Yang, Design and implementation of UWB planar monopole antenna with dual band rejection characteristics, Microwave Opt Technol Lett 54 (2012), 990–993.
4. W.X. Liu, Y.Z. Yin, and W.L. Xu, Design a new elliptical ultra wide band antenna with dual band-notched, Microwave Opt Technol Lett 54 (2012), 780–783.
5. X.J. Liao, H.C. Yang, N. Han, and Y. Li, UWB antenna with dual narrow band notches for lower and upper WLAN bands, Electron Lett 46 (2010), 1593–1594.
6. J. Kazim, A. Bibi, M. Rauf, and M. Tariq Owais, A compact planar dual band-notched monopole antenna for UWB application, Microwave Opt Technol Lett 56 (2014), 1095–1097.
7. W. Li, X. Shi, T. Zhang, and Y. Song, Novel UWB planar monopole antenna with dual band-notched characteristics, Microwave Opt Technol Lett 52 (2010), 48–51.

BANDPASS FILTER BASED ON NOVEL-COUPLED HALF-WAVELENGTH MICROSTRIP RING RESONATORS

Seyi S. Olokede,[1] Ihsan A. Zubir,[1] Mohd F. Ain,[1] and Zainal A. Ahmad[2]

[1] School of Electrical & Electronic Engineering, Universiti Sains Malaysia, 14300 Nibong Tebal, Penang, Malaysia; Corresponding author: solokede@gmail.com

[2] School of Material & Mineral Resources Engineering, Universiti Sains Malaysia, 14300 Nibong Tebal, Penang, Malaysia

Received 21 August 2015

ABSTRACT: *A microstrip bandpass filter (BPF) based on centre-coupled cylindrical microstrip ring resonator (MRR) for wireless application in ISM frequency band of applications is presented. The proposed is a combination of two identical bended half-wavelength (λ/2) MRR, and centre-coupled by an end-coupled transmission feed line. The equivalent circuits of the MRR, the end-coupled feed, and the effects of various spacing between them were investigated based on the even- and odd-mode theory. The mechanism of resonant mode splitting is investigated with the possibility of enhancing the coupling effect, while suppressing spurious resonances in order to achieve sharp rejection skirts. Findings indicates that the proposed equivalent circuit are influenced by capacitances due to resonator – transmission feed line gap (d), the gap between each ring (g), the feed line gap (i), the radius of MRR (r), and the resonator head (m). The operation mechanism of the structure was investigated first theoretically to the intent of design a circuit model, then using numerical 3D EM based on finite integration technique (FIT) method, and finally, through 2D equivalent circuit modeller. The derived equivalent circuit model have been validated both by analytical formulae and numerical simulations.* © 2016 Wiley Periodicals, Inc. Microwave Opt Technol Lett 58:911–918, 2016; View this article online at wileyonlinelibrary.com. DOI 10.1002/mop.29693

Key words: *bandpass filter; centred-coupled; even- and odd-mode theory; microstrip ring resonator*

1. INTRODUCTION

Over the years, MRR and its derivatives have been one of the burning issues in the RF, microwave and millimetre-wave systems community not only as microwave bandpass filters (BPF), couplers, mixers, oscillators, antennas, but even in applications involving complex permittivity measurements. One notable attractiveness of the MRRs that stand them out is first and foremost the increasing need for the optimum usage of space in modern microwave circuits. Low cost, sharp rejection skirts, high Q, compact size, light weight, microstrip modes, and low radiation loss for wireless communication are extra additives. In recent times, its material characterization attributes with ready applications in dielectric spectroscopy, has made them favorites for imaging biological samples [1,2], for soil moisture measurements [3], for cancer treatment [4], and this time not only for material measurement but also for circuit properties [5]. In Ref. 6, Liu & Pu introduced a concept of microwave chemistry using a novel MRR to measure complex permittivity of liquid. Subsequently, they are now common technology for filters design [7–16], antenna [16–19], and finally in oscillator circuits [20]. Seeing the proposed MRRs consist of sub-wavelength linear impedance sections of about quarter wavelength length, interaction between these components has been difficult to analyses in order to achieve accurate characterization as an ideal sub-wavelength linear impedance section is not realizable at lower frequencies because of the associated parasitic reactance due to fringing fields particularly by virtue of their electrical and physical lengths on assumption that: (1) the voltage across the linear impedance sections is constant at any point in the line, (2) the current just before and beyond the section are equal, which inadvertently leads to an infinitely short impedance sections [21].

However, these assumptions could not be ascertain as the geometric dimensions of these impedance sections result in a phase shift. Nonetheless, the effect of increasing the length of